

Analytical solutions for time-resolved fluorescence lifetime imaging in a turbid medium such as tissue

David Hattery

Laboratory of Integrative and Medical Biophysics, National Institute of Child Health and Human Development, National Institutes of Health, Building 12A, Room 2041, Bethesda, Maryland 20892, and Department of Electrical and Computer Engineering, Institute for Medical Imaging and Image Analysis, George Washington University, Washington, D.C. 20052

Victor Chernomordik

Laboratory of Integrative and Medical Biophysics, National Institute of Child Health and Human Development, National Institutes of Health, Building 12A, Room 2041, Bethesda, Maryland 20892

Murray Loew

Department of Electrical and Computer Engineering, Institute for Medical Imaging and Image Analysis, George Washington University, Washington, D.C. 20052

Israel Gannot

Biomedical Engineering Department, Faculty of Engineering, Tel-Aviv University, Tel-Aviv 69978, Israel

Amir Gandjbakhche

Laboratory of Integrative and Medical Biophysics, National Institute of Child Health and Human Development, National Institutes of Health, Building 12A, Room 2041, Bethesda, Maryland 20892

Received June 7, 2000; accepted December 6, 2000; revised manuscript received January 8, 2001

An analytical solution is developed to quantify a site-specific fluorophore lifetime perturbation that occurs, for example, when the local metabolic status is different from that of surrounding tissue. This solution may be used when fluorophores are distributed throughout a highly turbid media and the site of interest is embedded many mean scattering distances from the source and the detector. The perturbation in lifetime is differentiated from photon transit delays by random walk theory. This analytical solution requires *a priori* knowledge of the tissue-scattering and absorption properties at the excitation and emission wavelengths that may be obtained from concurrent time-resolved reflection measurements. Additionally, the solution has been compared with the exact, numerically solved solution. Thus the presented solution forms the basis for practical lifetime imaging in turbid media such as tissue. © 2001 Optical Society of America

OCIS codes: 170.3650, 170.5280, 170.6280.

1. INTRODUCTION

Fluorescence techniques have played a critical role in the description of biological processes at the molecular and cellular levels. Endogenous and exogenous fluorescent molecules are used as specific markers of metabolic status or disease processes.^{1–3} Fluorescent particles have been used as contrast agents for the study of transport phenomena (e.g., blood) in biological media.^{4–6} These successes were obtained in transparent media or in tissue when the markers were located close to the surface. Most biological tissues scatter light so strongly, however, that even special techniques to remove multiply scattered light (such as two-photon and confocal microscopies) fail at depths greater than 500 μm below the tissue surface. A complicating factor is the strong attenuation of light as

it passes through tissue which degrades the signal-to-noise ratio of detected photons. Fortunately, development of fluorescent dyes (such as porphyrin and cyanine) that excite and reemit in the “biological window” at near-infrared wavelengths, where scattering and absorption coefficients are relatively low, has opened new possibilities for deep fluorescence imaging in tissue. Further complication occurs at depths greater than 1 mm, where photons in most tissues enter a diffusionlike state with a large dispersion in their path lengths.^{7–11} Indeed, the fluorescent intensity collected from deep tissue structures depends not only on the location, size, concentration, and intrinsic characteristics (e.g., lifetime) of the fluorophores but also on the scattering and absorption coefficients of the tissue at both the excitation and the emission wave-

lengths. Hence, in order to extract intrinsic characteristics of fluorophores within tissue, it is necessary to describe the statistics of photon path lengths that depend on all of these differing parameters.

Obviously, the modeling of light propagation depends on the kinds of experiments that one plans to perform. For example, for steady-state (i.e., continuous-wave) measurements on a uniform distribution of fluorophore, approximations based on the Kubelka–Munk theory have been used.¹² For frequency-domain measurements, Patterson and Pogue¹³ and Sevik–Muraca and Burch¹⁴ used the diffusion approximation of the transport equation to express their results in terms of a product of two Green's function propagators multiplied by a term that describes the probability of emission of a fluorescent photon at the site. One Green's function describes the movement of a photon incident to the fluorophore, and the other describes movement of the emitted photon to the detector. In this representation, the amount of light emitted at the site of the fluorophore is directly proportional to the total amount of light impinging on the fluorophore, with no account made for the variability in the number of visits by a photon before an exciting transformation. Since a transformation on an early visit to the site precludes a transformation on all later visits, the result is an overestimation of the number of photons that have a fluorescence transformation at a particular site. This overestimation is important when fluorescent absorption properties are spatially inhomogeneous and largest at later arrival times. Gandjbakhche *et al.*¹⁵ have used random walk theory (RWT) to allow for this spatial inhomogeneity by introducing the multiple-passage probabilities concept, thus rendering the model more physically plausible. From these methods, analytical solutions were obtained for the case of frequency-domain measurements. For time-resolved fluorescence measurements, however, a closed-form, analytical solution for diffuse media has not been obtained.

The capability to quantify local changes in fluorescence lifetime in highly turbid media such as tissue is a potentially very powerful tool. By selecting fluorophore probes with known lifetime dependence on specific environmental variables, one can localize and quantify such metabolic parameters as temperature and pH, as well as changes in local molecular concentrations *in vivo*, by use of lifetime imaging. Lifetime-based methods do not require that the fluorophore be exclusively localized in the tissue of interest, as is required for intensity-based methods. Instead, the fluorophore lifetime changes in response to the tissue; for example, differing pH or oxygen content and the quantification of lifetime provides the necessary contrast.¹⁶ Since fluorescence probes can be minimally invasive, there is a strong incentive to tackle this problem and provide biomedical researchers a powerful new technique to probe functional processes in the body. Many researchers^{17–22} have designed numerical methods, such as finite-element models, to implement inverse algorithms based on local differential equations of the diffusion approximation to transport theory to quantify lifetime in turbid media from frequency-domain measurements. Although analytical solutions to diffusion theory are possible for a simple geometric configuration such as a

single spherical abnormal region in an otherwise-homogeneous infinite media,²³ most practical geometries require numerical solutions. Here, a general analytical method for obtaining site-specific fluorescence lifetime in semi-infinite media from time-resolved measurements is presented. Earlier work, using only early arriving photons, requires that the lifetime be long compared to the photon transit times,²⁴ which limits *in vivo* applications, because fluorophores that emit in the biological window in the near-infrared typically have very short lifetimes as compared with transit times for geometries of interest. Our method uses all photons, not just early arriving photons, and works when fluorescence lifetime is short compared with transit times and even for the case of spatially inhomogeneous fluorescent-based absorption. The derivation is based on RWT and requires knowledge of the average tissue absorption and scattering coefficients at both the fluorophore stimulation and the emission wavelengths. In practice, these coefficients may be obtained from time-resolved reflectance measurements at the same time that the time-resolved fluorescence data is collected. The analytical solution is compared with the numerically solved complete solution, and expected errors are less than 4%. This technique provides biomedical researchers a necessary tool to enable the use of time-resolved fluorescence lifetime techniques *in vivo*.

2. MODEL

To obtain information from discrete sites in tissue using fluorescence lifetime probes, one must generate a map of the tissue with lifetime values at each location. The derivation of our method for obtaining site-specific lifetime is divided into three steps. First, the effect of lifetime at a localized fluorophore site on photons arriving at a detector is shown. Next, a uniform distribution of fluorophores is assumed, and the aggregate fluorescent intensity at a detector is derived. Finally, the effect of a lifetime perturbation, originating at a localized site, on the global signal is presented. In practice, the map of tissue lifetime would be obtained by quantifying the local lifetime at numerous locations within the tissue.

For step one, a localized fluorophore site is assumed with fixed source and detector locations. To describe photon paths inside a highly scattering medium such as biological tissue, we use RWT on a lattice.¹⁰ On each step, the photon moves to one of the six closest lattice sites. The lattice spacing is proportional to the transport-corrected scattering distance, $1/\mu'_s$. Absorption is characterized by a dimensionless parameter $\mu = \mu_a/\mu'_s$ that expresses the probability of photon absorption on each step to an adjacent lattice site, and μ_a is the absorption coefficient of tissue.

In the probabilistic RWT model, the description of a photon path may be divided into three parts: the path from the photon source to a localized, fluorescing target; the interaction of the photon with the fluorophore; and finally, the path of the fluorescently emitted photon to a detector (see Fig. 1). Each part of the photon path may be described by a probability: first, the probability that an incident photon will arrive at the fluorophore site; second, the probability that the photon has a reactive encounter

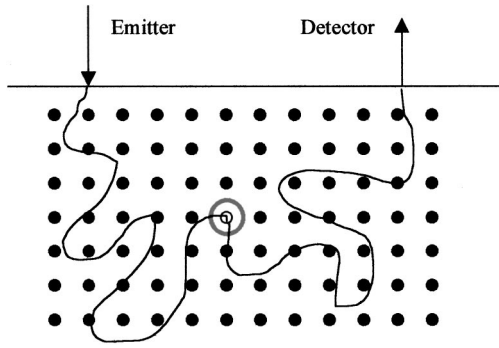


Fig. 1. 2D Random walk lattice showing representative photon paths from an emitter to a fluorophore site s and then to a detector r .

with the fluorophore and the corresponding photon transit delay, which is dependent on the lifetime of the fluorophore and the probability of the fluorophore emitting a photon; and third, the probability that the photon emitted by the fluorophore travels from the reaction site to the detector. Each of these three sequences is governed by a stochastic process.

Given a photon source located at r_0 , one may express the probability of a photon arriving at a particular site s in the tissue on step j as $p_j(s|r_0)$. If a fluorophore is placed at the particular site, there is a possibility that the fluorophore will be excited and later emit a photon. If this occurs, the photon will experience an en route delay of Δn steps while the fluorophore is in the excited state. It is convenient to consider the effect of the medium on the photon in two parts: a spatially homogeneous component and a site-specific differential component. The site with a differential component may be considered anomalous, and the effect of that anomaly is cumulative when the photon visits the site more than once. In general, for a stochastic model such as random walk, the cumulative effect of many individual probabilistic events, each described by δ , may be expressed as follows:

$$q_m = (1 - \delta)^{m-b} \delta^b, \quad \text{where} \quad \sum_{m=1}^{\infty} q_m = 1, \quad (1)$$

where m is the number of times a photon has visited the particular lattice site and b is a positive integer that is not greater than m . This formulation allows a dependence of a given event on previous events. Usually, one is interested in events that can happen only once and therefore must not have happened during all previous visits to the site, in which case $b = 1$. Absorption of a photon, such as when a fluorophore is excited, is one example, which may be expressed as $(1 - \eta)^{m-1} \eta$, where the constant η is the probability of absorption at each step n .²⁵ Another example is a fluorescence delay resulting from the excitation and later emission of a photon, which may be expressed as $(1 - \psi_k)^{m-1} \psi_k$, where the variable ψ_k is the probability of a delay of k steps. These two cases where $b = 1$ will be used together to describe fluorescence behavior.

Both of these anomalous effects only apply to the incident photons that exist at the fluorophore excitation wavelength. At this step we ignore reabsorption of the

fluorescently emitted photon on its travel to the detector, since this will be accounted for in step two. Since the number of times that an exciting wavelength photon has visited the site is used in Eq. (1), the term $f_j(s, m|r_0)$ will be used to denote the probability of a photon injected at r_0 visiting the anomalous site s at step j and that the photon has visited the site exactly m times—i.e., the first time a photon visits the site, or first-passage, $m = 1$, the second time, $m = 2$, etc. The trip from the fluorophore site to the detector after a fluorescent interaction may be expressed using the notation described earlier, $p'_{n-k-j}(r|s)$, where the prime denotes the fact that the wavelength of the emission photons is different from that of the incident photon. At the emission wavelength, the tissue scattering and absorption properties may be different, which affects the probability function. The subscript $n - k - j$ accounts for the fewer remaining steps the photon has to make from the fluorophore site to the detector as a result of both the fluorescent interaction and the number of steps before the fluorescent interaction. Putting all of the terms together, the probability of a photon being injected at r_0 resulting in a fluorescence photon being detected at r on step n that has experienced a delay k at a fluorophore site s may be expressed as follows:

$$\gamma(n, r, s, r_0) = \sum_{j=0}^n \sum_{m=1}^{\infty} (1 - \eta)^{m-1} \eta \Phi (1 - \psi_k)^{m-1} \times \psi_k f_j(s, m|r_0) p'_{n-k-j}(r|s), \quad (2)$$

where the probability that a photon will be absorbed by a fluorophore is η , and the fluorophore has a quantum efficiency Φ that describes the probability that if excited, the fluorophore will emit a photon at some later time. This efficiency is generally significantly less than one for most biological fluorophores.²⁶ The photon cannot visit the fluorophore site more times than there are steps in the path, i.e., $m \leq n$. Equivalently, all f_j where j is greater than n must be zero. Thus the summation is in practice finite. Equation (2) is an exact representation of the probability of a fluorescence photon arriving at a detector and does not place any restrictions on the magnitude and probability distributions of either photon absorption or fluorescence delays at the site.

Since the summation in Eq. (2) is in the form of a convolution, it is generally preferable to use generating functions where the transform is an analog of the Laplace transform for a discrete summation with transform variable ξ :

$$\hat{g}_{\xi} = \sum_{n=0}^{\infty} g_n \exp(-n\xi) \equiv L_n\{g_n\}. \quad (3)$$

Applying the transformation to Eq. (2), one obtains

$$\hat{\gamma}(r, s, r_0) = \eta \Phi \hat{\psi} \hat{p}'_{\xi}(r|s) \sum_{m=1}^{\infty} (1 - \hat{\psi}_k)^{m-1} \times (1 - \eta)^{m-1} \hat{f}_{\xi}(s, m|r_0). \quad (4)$$

To solve this equation, one must examine the last term, or multiple-passage probability. The probability of a pho-

ton arriving at the fluorophore site in n steps may be expressed as the product of the probability of a photon arriving at the site for the first time at step j (first-passage probability) and returning to the site in $n - j$ steps. This may be expressed as follows:

$$p_n(s|r_0) = \sum_{j=0}^n f_j(s, 1|r_0)p_{n-j}(s|s), \quad (5)$$

where the probability of a photon returning to the site at a later time is the recirculation probability, which is denoted $p_{n-j}(s|s)$. Since Eq. (5) is in the form of a convolution, the transform defined by Eq. (3) may be used to solve for the first-passage probability, which is then

$$\hat{f}_\xi(s, 1|r_0) = \hat{p}_\xi(s|r_0)/\hat{p}_\xi(s|s). \quad (6)$$

To solve for passage probabilities greater than the first, a recursive method is used that is based on the following relationship:

$$f_n(s, m+1|r_0) = \sum_{j=0}^n f_j(s, m|r_0)f_{n-j}(s, 1|r_0). \quad (7)$$

Again by using the generating function in Eq. (3), we may show the multiple-passage probability to be

$$\hat{f}_\xi(s, m|r_0) = \hat{f}_\xi(s, 1|r_0)[\hat{f}_\xi(s, 1|s)]^{m-1}. \quad (8)$$

When we convert the multiple-passage to passage-

which is the result for frequency-domain measurements obtained by Patterson and Pogue¹³ and Sevvick-Muraca and Burch.¹⁴ This model allows photons that have had a previous fluorescent transformation to have another transformation at the same site on a later visit and thus overestimates the number of fluorescent photons. This overestimation is most significant at late arrival times and when the site's fluorescence absorption (local fluorophore concentration) is high.

To continue working with Eq. (10), it is necessary to consider the model for the fluorescence delay at the site. Since time delays that are due to fluorescence follow an exponential, one may use a more general expression for the probability of a particular delay k , which in discrete terms is shown with its generating function

$$\psi_k = (1 - \theta)\theta^{k-1} \Rightarrow \hat{\psi} = \frac{1 - \theta}{\exp(\xi) - \theta}, \quad (13)$$

where θ is a real number between 0 and 1 and k is a positive integer. The mean delay is then $(1 - \theta)^{-1}$, which will be denoted as $\langle \Delta n \rangle$. For fluorophore sites greater than a few lattice distances from a boundary, the multiple-passage probability has been shown to be¹⁵:

$$\hat{p}_\xi(s|s) \approx 1 + \frac{1}{8} \left(\frac{3}{\pi} \right)^{3/2} \sum_{j=1}^{\infty} \frac{\exp(-2j\xi)}{j^{3/2}}. \quad (14)$$

Inserting Eqs. (13) and (14) into Eq. (10) yields the complete solution for the probability of fluorescence photon arrival at the detector,

$$\hat{\gamma}(r, s, r_0) = \frac{\eta \Phi \hat{p}'_\xi(r|s) \hat{p}_\xi(s|r_0)}{\langle \Delta n \rangle (1 - \eta) [\exp(\xi) - 1] + \{ \eta \langle \Delta n \rangle [\exp(\xi) - 1] + 1 \} \left[1 + \left[\frac{1}{8} \left(\frac{3}{\pi} \right)^{3/2} \sum_{j=1}^{\infty} \frac{\exp(-2j\xi)}{j^{3/2}} \right] \right]}. \quad (15)$$

independent terms by using Eq. (6), it becomes

$$\hat{f}_\xi(s, m|r_0) = \frac{\hat{p}_\xi(s|r_0)}{\hat{p}_\xi(s|s)} \left[1 - \frac{1}{\hat{p}_\xi(s|s)} \right]^{m-1}. \quad (9)$$

Substituting into Eq. (4) and solving for the summation yields the general expression for the probability of fluorescence arrival at a detector,

$$\begin{aligned} \hat{\gamma}(r, s, r_0) &= \frac{\eta \Phi \hat{p}'_\xi(r|s) \hat{p}_\xi(s|r_0)}{(1 - \hat{\psi})(1 - \eta) + [1 - (1 - \hat{\psi})(1 - \eta)] \hat{p}_\xi(s|s)}. \end{aligned} \quad (10)$$

If the requirement for all previous and subsequent passages to be nonfluorescing is removed, the total probability of a fluorescence even is the summation of Eq. (9) from $m = 1$ to infinity,

$$\sum_{m=1}^{\infty} \frac{\hat{p}_\xi(s|r_0)}{\hat{p}_\xi(s|s)} \left[1 - \frac{1}{\hat{p}_\xi(s|s)} \right]^{m-1} = \hat{p}_\xi(s|r_0). \quad (11)$$

In this case, Eq. (4) becomes

$$\hat{\gamma}(r, s, r_0) = \eta \Phi \hat{\psi} \hat{p}'_\xi(r|s) \hat{p}_\xi(s|r_0), \quad (12)$$

In practice, this solution is difficult to work with, so some simplifying assumptions are desired. Assuming that the multiple passage probability is one—the photon has an equal probability for a fluorescent interaction on each visit to the inclusion site—Eq. (15) simplifies to

$$\hat{\gamma}(r, s, r_0) = \frac{\eta \Phi \hat{p}'_\xi(r|s) \hat{p}_\xi(s|r_0)}{\langle \Delta n \rangle [\exp(\xi) - 1] + 1}. \quad (16)$$

For small ξ , ($\xi \ll 1/\langle \Delta n \rangle$), one may make further simplifications. The small ξ assumption is reasonable for fluorescence imaging of deeply embedded sites in tissue and requires that photon transit times be long compared to the fluorophore lifetime. Making this approximation and using the first two terms of the exponential in the denominator of Eq. (16), one obtains:

$$\begin{aligned} \hat{\gamma}(r, s, r_0) &= \eta \Phi \{ \hat{p}'_\xi(r|s) \hat{p}_\xi(s|r_0) \\ &\quad - \xi \langle \Delta n \rangle \hat{p}'_\xi(r|s) \hat{p}_\xi(s|r_0) \}. \end{aligned} \quad (17)$$

W_n is defined as the inverse of the transform defined in Eq. (3) of the product of the two transit probability terms as follows:

$$W_n \equiv L_n^{-1} [\hat{p}'_\xi(r|s) \hat{p}_\xi(s|r_0)]. \quad (18)$$

For the case where the tissue-scattering and absorption properties are the same for all paths, W_n has been described²⁷ as behaving like a time-dependent spatial point-spread function (PSF) of an imaging system. In this case, however, the scattering and absorption properties change when fluorescence changes the photon wavelength, as indicated by the prime on the first term in Eq. (18). Applying the inverse transform to Eq. (17) and noting that

$$W_n - W_{n-1} = L_n^{-1}\{\xi W_n\}, \quad (19)$$

one obtains

$$\gamma(n, r, s, r_0) = \eta \Phi[W_n - \langle \Delta n \rangle (W_n - W_{n-1})]. \quad (20)$$

The $W_n - W_{n-1}$ term is the discrete version of a derivative. To convert to real-world variables, the following relationships are used: $n = ct\mu'_{si}$, $r = r'\mu'_{si}/2^{1/2}$, $r_0 = r'_0\mu'_{si}/2^{1/2}$, and $\eta = \mu_{af}/\mu'_{si}$, where μ_{af} is the probability of absorption by a fluorophore, μ'_{si} is the transport-corrected scattering coefficient for photons at the excitation wavelength, t is time, and c is the speed of light in tissue. The probability of arrival function, in the real world variables of, t , s' , r'_0 , and r' , may be expressed as follows:

$$\gamma(t, r', s', r'_0) = \frac{\mu_{af}}{\mu'_{si}} \Phi \left(W_t - \langle \Delta t \rangle c \mu'_{si} \frac{dW_t}{dt} \right). \quad (21)$$

The effect of a short en route delay, Δt , at the fluorophore site is contained the second term, where the mean delay is multiplied by the time derivative of the PSF. The fluorescence delay at the site may have any statistical form that satisfies Eq. (13), and the only parameter that affects photon probability of arrival at a detector is the mean delay. Furthermore, the mean delay at the fluorophore site is the fluorescence lifetime, τ .

To analyze Eq. (21), the PSF elements are expanded as Green's functions with four elements^{15,27}:

$$W_t = h(\alpha_-, \beta_-) - h(\alpha_-, \beta_+) - h(\alpha_+, \beta_-) + h(\alpha_+, \beta_+). \quad (22)$$

The dimensionless parameters α are functions of the distance from a photon source, which is located at the origin, to a fluorophore site centered at the mean (x_f, y_f, z_f) point, as illustrated in Fig. 2:

$$\alpha_{\pm} = \frac{3}{4} \left[\bar{x}_f^2 + \bar{y}_f^2 + \left(\bar{z}_f \pm \frac{\sqrt{2}}{\mu'_{si}} \right)^2 \right] \mu'^2_{si}. \quad (23)$$

The minus and plus components may be interpreted as the respective distances from the actual source and its image across the tissue-air boundary. Similarly, the dimensionless parameters β are functions of the distance from the fluorophore site to a detector located at the point $(x, y, 0)$.

$$\beta_{\pm} = \frac{3}{4} \left[(\bar{x}_f - x)^2 + (\bar{y}_f - y)^2 + \left(\bar{z}_f + \frac{\sqrt{2}}{\mu'_{se}} \pm \frac{\sqrt{2}}{\mu'_{se}} \right)^2 \right] \mu'^2_{se}, \quad (24)$$

where μ'_{se} is the transport-corrected scattering coefficient for photons at the fluorophore emission wavelength. If one assumes that the absorption coefficients in tissue at the excitation and emission wavelengths are the same, the PSF has a closed-form solution. More practically,

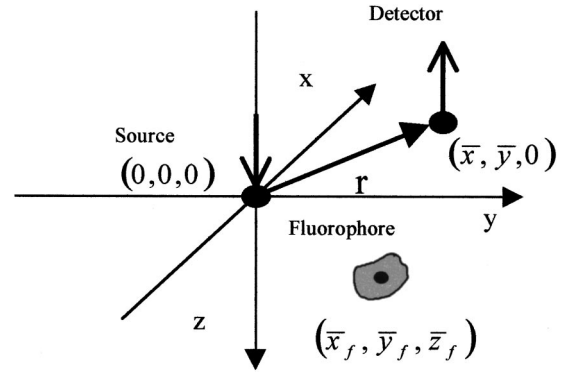


Fig. 2. Imaging geometry showing the relative locations of the photon source, fluorophore site s , and detector r .

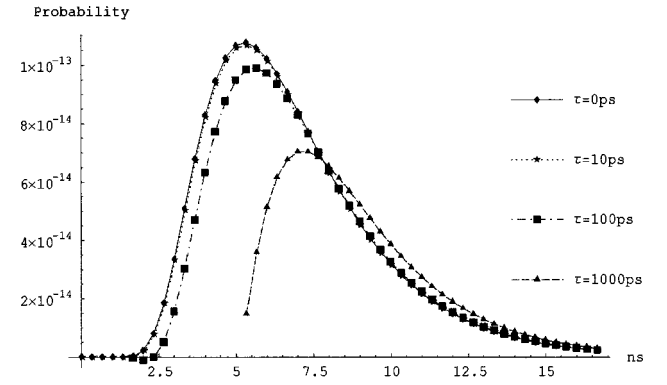


Fig. 3. Dependence on probable time-of-photon-arrival for fluorophore lifetimes of 0, 10, 100, and 1000 ps with source at origin, detector at (30, 0, 0 mm), fluorophore at (15, 0, 8 mm), scattering $\mu'_s = 1/\text{mm}$, and absorption 0.001/mm at both excitation and emission wavelengths.

one may use the average absorption $\mu_a = (\mu_{ae} + \mu_{ai})/2$ where μ_{ae} and μ_{ai} are the absorption coefficients at the emission and excitation wavelengths respectively. The PSF may then be constructed using

$$h(\alpha, \beta) = \frac{\sqrt{\alpha} + \sqrt{\beta}}{[ct(\mu'_{si}\mu'_{se})^{1/2}]^{3/2}(\pi\alpha\beta)^{1/2}} \times \exp \left(-\frac{\sqrt{\alpha} + \sqrt{\beta}}{ct(\mu'_{si}\mu'_{se})^{1/2}} - ct\mu_a \right). \quad (25)$$

It should be noted that the different scattering coefficients of the excitation-wavelength photons and the fluorescently emitted photons, and thus the effect of those differences, are also contained in the α and β terms. Similarly, the derivative of the PSF may be constructed using the same form as in Eq. (22) by replacing the h terms with

$$h'(\alpha, \beta) = \frac{(\sqrt{\alpha} + \sqrt{\beta})(2\alpha + 4\sqrt{\alpha\beta} + 2\beta - 3ct\sqrt{\mu'_{si}\mu'_{se}})}{2(ct\sqrt{\mu'_{si}\mu'_{se}})^{7/2}\sqrt{\pi\alpha\beta}} \times \exp \left(-\frac{(\sqrt{\alpha} + \sqrt{\beta})^2}{ct(\mu'_{si}\mu'_{se})^{1/2}} - ct\mu_a \right). \quad (26)$$

Expanding Eq. (21) using the elements in Eqs. (22)–(26), one obtains

$$\gamma(t, r', s') = \frac{\mu_{af}}{\mu'_{si}} \Phi \left\{ \begin{aligned} &h(\alpha_-, \beta_-) - h(\alpha_-, \beta_+) - h(\alpha_+, \beta_-) + h(\alpha_+, \beta_+) \\ &- \tau c \mu'_{si} [h'(\alpha_-, \beta_-) - h'(\alpha_-, \beta_+) - h'(\alpha_+, \beta_-) + h'(\alpha_+, \beta_+)] \end{aligned} \right\}. \quad (27)$$

In Fig. 3, plots of Eq. (27) illustrate the change in the location of the mode time-of-arrival resulting from changes in fluorophore lifetime. As expected, longer lifetimes move the mode to later times.

The use of an average absorption in Eqs. (25) and (26) is not as limiting as one might expect on the basis of the observation that although the scattering coefficient changes relatively slowly as a function of wavelength, absorption in tissue can change very quickly; localized absorption peaks in the spectrum are common. Expected maximum errors for the cases where there are twofold and fourfold differences in absorption coefficients are illustrated in Fig. 4 and can be shown to occur less than 10 percent at the time at which the probability of arrival is maximum (mode time). This small error, despite a large change in absorption, is due to the dominating effect of scattering, which in the near infrared is 100–1000 times greater than absorption.²⁸ Furthermore, the effect of the error in absorption is a reduction in intensity that is greatest near and after the mode time, and is very small for early arriving photons. The effect of a change in lifetime, however, is largest where the derivative of the PSF is largest. The derivative is largest at early times when the effect of an error in absorption is small. Thus combining the absorption coefficients of two wavelengths into a single term should have minimal effect on the extraction of lifetime.

In step two, the probability of photon arrivals is derived for the case where fluorophores are uniformly distributed throughout the volume of tissue. Simply performing a spatial integration of isolated fluorophore sites as described in step one will not work, because the uniform distribution of fluorophores makes it possible that a fluorophore, otherwise destined for a fluorescent interaction at one site, will have a fluorescent interaction at an earlier site. Since typical fluorescent interactions transform photons from one wavelength to another that is much less likely to be involved in a fluorescent interaction, the process is similar to non-fluorescence-based absorption in tissue. An effective, or fluorescence-corrected absorption term, which is denoted by a prime, is introduced for both the exciting and the emitted wavelengths as follows:

$$\mu'_{ai} = \mu_{ai} + \mu_{af} \quad \mu'_{ae} = \mu_{ae} + \mu_{afe}, \quad (28)$$

where the new term μ_{afe} is the probability of fluorescence reabsorption. This simple form of quenching becomes significant at concentrations of fluorophores high enough to significantly increase the probability that emission-wavelength photons are reabsorbed, thereby reducing the number of fluorescent photons that reach the detector.²⁶

The background fluorescence lifetime signal can then be solved by integrating Eq. (21) over all possible sites, s' , in the volume. The solution is

$$\gamma(t, r') = \frac{\mu_{af}}{\mu'_{si}} \Phi \left[P(t, r') - \langle \Delta t \rangle c \mu'_{si} \frac{dP(t, r')}{dt} \right], \quad (29)$$

where $p(t, r')$ is the probability of a photon arriving at point r' at time t absent any fluorescence behavior. Making a similar assumption as before and using the average absorption, $\mu'_a = (\mu'_{ae} + \mu'_{ai})/2$, in the diffuse reflectance formula for a thick, semi-infinite slab¹⁰ one obtains

$$\begin{aligned} p(t, r') = & \frac{\sqrt{3}}{2} \left\{ \frac{1}{2\pi[ct(\mu'_{si}\mu'_{se})^{1/2} - 2]} \right\}^{3/2} \\ & \times \exp \left\{ \frac{-3\mu'_{si}\mu'_{se}r'^2}{4[ct(\mu'_{si}\mu'_{se})^{1/2} - 2]} \right\} \\ & \times \left\{ 1 - \exp \left[\frac{-6}{ct(\mu'_{si}\mu'_{se})^{1/2} - 2} \right] \right\} \exp(-\mu'_a ct). \end{aligned} \quad (30)$$

Finally, in step three the effect of a perturbation in the delay of photons fluorescing at a specific localized site is isolated to distinguish it from the background fluorescence lifetime. In this step, we assume that spatial variations in emission intensity, or contrast, measured on the tissue surface result from differing lifetimes of the fluorophore within the tissue. Contrast may be defined as

$$C(t, r') = \frac{I(t, r') - \langle I(t) \rangle}{\langle I(t) \rangle}, \quad (31)$$

where intensity at the fluorophore emission wavelength, $I(t, r')$, is measured at a particular point on the tissue surface at a specific time relative to a pulse of photons at the excitation wavelength. The other term, $\langle I(t) \rangle$, is the

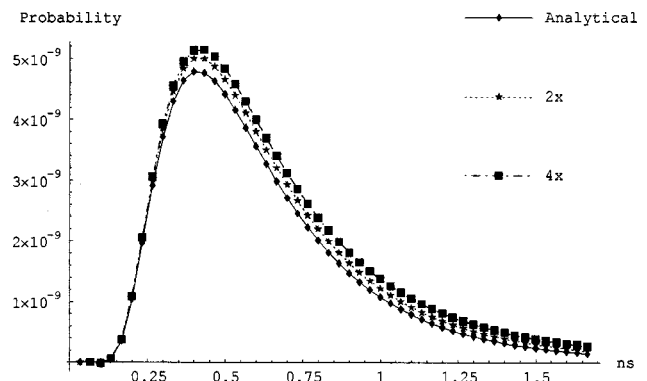


Fig. 4. Comparison between the analytical solution and two numerically solved exact solutions using Eq. (15) for a typical worst-case geometry [asymmetrically placed fluorophore directly under the detector, source at origin, detector at (10, 0, 0 mm), and 10 ps lifetime fluorophore at (10, 0, 10 mm)] with scattering $\mu'_s = 1/\text{mm}$. The analytical solution uses an average absorption of 0.005/mm. The exact 2× case uses $\mu_{ai} = 0.0033/\text{mm}$ and $\mu_{ae} = 0.0067/\text{mm}$, and the exact 4× case uses $\mu_{ai} = 0.002/\text{mm}$ and $\mu_{ae} = 0.008/\text{mm}$.

average spatial intensity at the emission wavelength as a function of time. Contrast may also be considered the sum of contributions from each site in the tissue as follows:

$$C(t, r') = \sum_{s'} C_{s'}(t, r', s'). \quad (32)$$

The contrast from each site is a function of the difference between the mean lifetime of the fluorophore in the tissue, $\langle\tau\rangle$, and the local lifetime at the site of interest, $\tau_{s'}$. From Eqs. (21) and (29),

$$C_{s'}(t, r', s') = \frac{(\langle\tau\rangle - \tau_{s'})}{p(t, r')} \frac{dW_{t,s'}}{dt}, \quad (33)$$

where the subscript s' on the PSF derivative indicates that each site will have a unique PSF. The average fluorescence-corrected absorption μ'_a is used to compute the PSF. One may take advantage of the fact that the PSF, which is the inverse Laplace transform of the product of two site-specific Green's functions, is highly nonlinear as one changes sites in the tissue. Thus the component of total contrast that is linear with respect to the time derivative of a site-specific PSF normalized by $p(t, r')$ is an estimate of $(\langle\tau\rangle - \tau_{s'})$, which is the lifetime perturbation at the specific site in the tissue. From Eqs. (29) and (30) one may obtain the mean lifetime, or delay $\langle\tau\rangle \equiv \langle\Delta t\rangle$. From this, an estimate of the site-specific lifetime, $\tau_{s'}$, is obtained.

The inverse solution requires one to analytically calculate the value of the PSF, which requires knowledge of the absorption and scattering coefficients at the two wavelengths. In practice, estimates of these parameters may be obtained through use of time-resolved reflectance measurements¹⁰ by adding a source at the fluorophore emission wavelength and adding detectors that take measurements at the fluorophore stimulation wavelengths. With use of the second source with the existing detectors, fluorescence-corrected absorption and scattering coefficients may be obtained at the fluorophore emission wavelength. Similarly, with use of the original source and taking measurements with the second set of detectors, fluorescence corrected absorption and scattering coefficients may be obtained at the fluorophore simulation wavelength. These additional two sets of measurements provide the information required to compute the PSF and therefore the site-specific lifetime perturbation. A lifetime map may be constructed by repeating this process and using the PSF for other locations in the tissue.

3. DISCUSSION

Fluorescence lifetime imaging may be used to obtain functional information from local concentrations of specific substances, such as O_2 , or information about metabolic-dependent environmental conditions, such as temperature and pH. Quantification, with lifetime techniques, requires a fluorophore with a known dependence on the environmental factor of interest. For deeply embedded sites in a turbid medium such as tissue, measuring the photon arrival delay caused by a specific fluorophore lifetime is made difficult by the photon arrival delays that re-

sult from multiple scattering of photons on their transit through tissue. To separate the two sources of delays (lifetime delays and scattering delays), a theory describing the delays caused by the scattering of photons in tissue is required. RWT has proven capable of describing the distribution of path lengths and therefore the amount of scattering experienced by photons traveling between two points in tissue. The delay of photons that results from the excitation of and subsequent emission by a fluorophore may be modeled in RWT as an en route delay that can be isolated from transit delays caused by multiple scattering. Thus the RWT is well suited to solving this type of problem.

A RWT-based analytical solution for time-resolved fluorescence lifetime imaging has been shown. Derivation of this solution required one fundamental assumption: that minimal error results from the substitution of the average excitation and emission wavelength absorption coefficients for the two separate coefficients. This substitution was required to express the solution in closed form. Whereas the scattering coefficient is relatively constant for near-infrared photons, the absorption can vary substantially. This assumption was shown to have relatively little effect, because the photon-scattering coefficients are 100–1000 times larger and dominate the solution. Thus a change in the absorption coefficient by a factor of four results in less than 10% change in the number of photon arrivals at the mode time and a factor of two change results in only 3–4% error. By comparison, a change of 7.4% in the line-of-sight distance traveled by those photons would result in a factor-of-two change in the peak number of arrivals.

Furthermore, when fluorophore lifetime is changed the number of photon arrivals at the mode time does not change, but there is a corresponding shift in the mode time. Lifetime imaging looks for changes in the statistics that describe the arrival times of photons at a detector. Since the error caused by averaging the absorption coefficients results primarily in an amplitude error that is very small where the derivative of the PSF is large, determination of lifetime will be minimally affected by this error. Therefore this closed-form solution provides a practical basis for time-resolved fluorescence lifetime imaging.

To solve for the case in which fluorophores are distributed throughout the tissue, an effective absorption term was introduced. This term takes advantage of the similarity between tissue absorption and fluorescence interactions. The fundamental assumption, described previously, was used again with this effective absorption to show an analytical solution for the background component of fluorescence lifetime imaging. Finally, a perturbation method was used to isolate the effect of a localized difference in lifetime from the background. Isolating the site-specific lifetime in this complex case in which fluorophores are distributed throughout a highly scattering medium is possible given an analytical solution such as the one presented. The solution requires computation of the PSF for each location of interest in the tissue. This further requires knowledge of the scattering and absorption coefficients of the tissue at the excitation and emission wavelengths of the fluorophore. Thus measurements of the optical tissue properties, such as those based on time-

resolved reflectance, must be made before this analytical solution to lifetime imaging may be applied. Since these measurements may be obtained by incorporating a second source at the fluorophore emission wavelength and detectors at the fluorophore stimulation wavelength, all required information may be obtained nearly simultaneously. The existence of this analytical solution makes it possible to perform time-resolved lifetime imaging, where local differences in lifetime are spatially resolved in highly scattering media. The authors intend to form a collaboration with researchers having experimental expertise to test specific applications of this theory.

ACKNOWLEDGMENTS

David Hattery is grateful for support from the Achievement Rewards for College Scientists (ARCS) Foundation. Amir Gandjbakhche and Israel Gannot wish to thank the American Israeli Binational Foundation (BSF) for its support.

Corresponding author David Hattery can be reached at the address on the title page or by e-mail at hatteryd@mail.nih.gov.

REFERENCES

- G. A. Wagnieres, W. M. Star, and B. C. Wilson, "In vivo fluorescence spectroscopy and imaging for oncological applications," *Photochem. Photobiol.* **68**, 603–632 (1998).
- M. Gurfinkel, A. B. Thompson, W. Ralston, T. L. Troy, A. L. Moore, T. A. Moore, J. D. Gust, D. Tatman, J. S. Reynolds, B. Muggenburg, K. Nikula, R. Pandey, R. H. Mayer, D. J. Hawrysz, and E. M. Sevick-Muraca, "Pharmacokinetics of ICG and HPPH-car for the detection of normal and tumor tissue using fluorescence, near-infrared reflectance imaging: a case study," *Photochem. Photobiol.* **72**, 94–102 (2000).
- R. Weissleder, C. H. Tung, and U. Mahmood, "In vivo imaging of tumors with protease-activated near-infrared fluorescent probes," *Nat. Biotechnol.* **17**, 375–378 (1999).
- R. Cubeddu, G. Canti, M. Musolino, A. Pifferi, P. Taroni, and G. Valentini, "In vivo absorption spectrum of disulphonated aluminium phthalocyanine in a murine tumour model," *J. Photochem. Photobiol. B* **34**, 229–235 (1996).
- C. Klinteberg, A. M. K. Enejder, I. Wang, S. Andersson-Engels, S. Svanberg, and K. Svanberg, "Kinetic fluorescence studies of 5-aminolaevulinic acid-induced protoporphyrin IX accumulation in basal cell carcinomas," *J. Photochem. Photobiol. B* **49**, 120–128 (1999).
- K. Dowling, M. J. Dayel, S. C. W. Hyde, P. M. W. French, M. J. Lever, J. D. Hares, and A. K. L. Dymoke-Bradshaw, "High resolution time-domain fluorescence lifetime imaging for biomedical applications," *J. Mod. Opt.* **46**, 199–206 (1999).
- R. F. Bonner, R. Nossal, S. Havlin, and G. H. Weiss, "Model for photon migration in turbid biological media," *J. Opt. Soc. Am. A* **4**, 423–432 (1987).
- A. H. Gandjbakhche, R. Nossal, and R. F. Bonner, "Resolution limits for optical transillumination of abnormalities embedded in tissues," *Med. Phys.* **22**, 185–191 (1994).
- J. A. Moon and J. Reintjes, "Image resolution by use of multiply scattered light," *Opt. Lett.* **19**, 521–523 (1994).
- A. H. Gandjbakhche and G. H. Weiss, "Random walk and diffusion-like model of photon migration in turbid media," in *Progress in Optics*, E. Wolf, ed. (Elsevier North-Holland, Amsterdam, 1995), Vol. 34, pp. 333–402.
- E. M. Sevick-Muraca and C. Hutchinson, "Probability description of fluorescent and phosphorescent signal generation in tissues and other random media," in *Advances in Laser and Light Spectroscopy to Diagnose Cancer and Other Diseases*, R. R. Alfano, ed., Proc. SPIE **2387**, 62–70 (1995).
- J. Wu, M. S. Feld, and R. P. Rava, "Analytical model for extracting intrinsic fluorescence in turbid media," *Appl. Opt.* **32**, 3585–3595 (1993).
- M. S. Patterson and B. Pogue, "A mathematical model for time-resolved and frequency-domain fluorescence spectroscopy in biological tissue," *Appl. Opt.* **33**, 1963 (1994).
- E. M. Sevick-Muraca and C. L. Burch, "Origin of phosphorescence signals reemitted from tissues," *Opt. Lett.* **19**, 1928–1930 (1994).
- A. H. Gandjbakhche, R. F. Bonner, R. Nossal, and G. H. Weiss, "Effects of multiple-passage probabilities on fluorescent signals from biological media," *Appl. Opt.* **36**, 4613–4619 (1997).
- D. Y. Paithankar, A. U. Chen, B. W. Pogue, M. S. Patterson, and E. M. Sevick-Muraca, "Imaging of fluorescent yield and lifetime from multiply scattered light reemitted from random media," *Appl. Opt.* **36**, 2260–2272 (1997).
- C. L. Hutchinson, J. R. Lakowicz, and E. M. Sevick-Muraca, "Fluorescence lifetime-based sensing in tissues: a computational study," *Biophys. J.* **68**, 1574–1582 (1995).
- J. S. Reynolds, T. L. Troy, R. H. Mayer, A. B. Thompson, D. J. Waters, K. K. Cornell, P. W. Snyder, and E. M. Sevick-Muraca, "Imaging of spontaneous canine mammary tumors using fluorescent contrast agents," *Photochem. Photobiol.* **70**, 87–94 (1999).
- R. H. Mayer, J. S. Reynolds, and E. M. Sevick-Muraca, "Measurement of the fluorescence lifetime in scattering media by frequency-domain photon migration," *Appl. Opt.* **38**, 4930–4938 (1999).
- D. Y. Paithankar and E. M. Sevick-Muraca, "Fluorescence lifetime imaging with frequency-domain photon migration measurement," in *Biomedical Optical Spectroscopy and Diagnostics*, E. Sevick-Muraca and D. Benaron, eds., Vol. 3 of OSA Trends in Optics and Photonics Series (Optical Society of America, Washington, DC, 1996), pp. 184–194.
- H. Jiang, "Frequency-domain fluorescent diffusion tomography: a finite-element-based algorithm and simulations," *Appl. Opt.* **37**, 5337–5343 (1998).
- A. E. Cerussi, J. S. Maier, S. Fantini, M. A. Franceschini, W. W. Mantulin, and E. Gratton, "Experimental verification of a theory for the time-resolved fluorescence spectroscopy of thick tissues," *Appl. Opt.* **36**, 116–124 (1997).
- X. D. Li, M. A. O'Leary, D. A. Boas, B. Chance, and A. G. Yodh, "Fluorescent diffuse photon density waves in homogeneous and heterogeneous turbid media: analytic solutions and applications," *Appl. Opt.* **35**, 3746–3758 (1996).
- J. Wu, Y. Wang, and L. Perelman, "Three-dimensional imaging of objects embedded in turbid media with fluorescence and Raman spectroscopy," *Appl. Opt.* **34**, 3425–3430 (1995).
- A. H. Gandjbakhche, R. F. Bonner, R. Nossal, and G. H. Weiss, "Absorptivity contrast in transillumination imaging of tissue abnormalities," *Appl. Opt.* **35**, 1767–1774 (1996).
- J. R. Lakowicz, *Principles of Fluorescence Spectroscopy*, 2nd ed. (Kluwer Academic/Plenum, New York, 1999).
- A. H. Gandjbakhche, V. Chernomordik, J. C. Hebden, and R. Nossal, "Time-dependence contrast functions for quantitative imaging in time-resolved transillumination experiments," *Appl. Opt.* **37**, 1973–1981 (1998).
- R. R. Anderson and J. A. Parrish, "The optics of human skin," *J. Invest. Derm.* **77**, 13–19 (1981).